Cationic DMPC/DMTAP Lipid Bilayers: Molecular Dynamics Study

Andrey A. Gurtovenko,*[†] Michael Patra,[‡] Mikko Karttunen,[‡] and Ilpo Vattulainen*

*Laboratory of Physics and Helsinki Institute of Physics, Helsinki University of Technology, FIN-02015 HUT, Finland;
[†]Institute of Macromolecular Compounds, Russian Academy of Sciences, St. Petersburg, 199004 Russia; and
[‡]Biophysics and Statistical Mechanics Group, Laboratory of Computational Engineering, Helsinki University of Technology, FIN-02015 HUT, Finland

ABSTRACT   Cationic lipid membranes are known to form compact complexes with DNA and to be effective as gene delivery agents both in vitro and in vivo. Here we employ molecular dynamics simulations for a detailed atomistic study of lipid bilayers consisting of a mixture of cationic dimyristoyltrimethylammonium propane (DMTAP) and zwitterionic dimyristoylphosphatidylcholine (DMPC). Our main objective is to examine how the composition of the DMPC/DMTAP bilayers affects their structural and electrostatic properties in the liquid-crystalline phase. By varying the mole fraction of DMTAP, we have found that the area per lipid has a pronounced nonmonotonic dependence on the DMTAP concentration, with a minimum around the point of equimolar DMPC/DMTAP mixture. We show that this behavior has an electrostatic origin and is driven by the interplay between positively charged TAP headgroups and the zwitterionic phosphatidylcholine (PC) heads. This interplay leads to considerable reorientation of PC headgroups for an increasing DMTAP concentration, and gives rise to major changes in the electrostatic properties of the lipid bilayer, including a significant increase of total dipole potential across the bilayer and prominent changes in the ordering of water in the vicinity of the membrane. Moreover, chloride counterions are bound mostly to PC nitrogens implying stronger screening of PC heads by Cl ions compared to TAP headgroups. The implications of these findings are briefly discussed.

INTRODUCTION

Gene therapy based on the introduction of genetic material into cells is one of the most promising biomedical approaches to treat human diseases (de Gennes, 1999; Langer, 1998; Mönkkönen and Urtti, 1998). The majority of the delivery vectors proposed are of viral nature. The viral vectors have been demonstrated to be very efficient but their use is restricted by accompanied toxicity (Anderson, 1998). This has stimulated a search for nonviral delivery systems, which should be characterized by greater safety and ease of manufacturing (Langer, 1998). Numerous examples of nonviral delivery vectors include cationic liposomes, cationic polymers (such as polyamidoamine dendrimers, polyethylenimine, and spermine), and block copolymers (Astafieva et al., 1996; Fischer et al., 1999; Gao and Huang, 1996; Kukowska-Latallo et al., 1996; Mönkkönen and Urtti, 1998; Pitard et al., 1997; Smedt et al., 2000).

In the light of the above, it is surprising how little attention has been devoted to computational studies of membranes containing cationic lipids. Bandyopadhyay et al. (1999) performed an atomistic molecular dynamics (MD) study of a mixture of dimyristoylphosphatidylcholine (DMPC) and dimyristoyltrimethylammonium propane (DMTAP) in the presence of a short DNA fragment. Apart from the very elegant piece of work above, there are, to the best of our knowledge, no published atomistic computational studies of systems containing cationic lipids—this is very much in contrast to the great number of computational studies of various neutral and anionic phospholipid bilayer systems (Feller, 2000; Saiz et al., 2002; Saiz and Klein, 2002; Tieleman et al., 1997; Tobias, 2001). Another related example is the recent molecular dynamics study of Böckmann et al. (2003), who showed the importance of monovalent ions on the properties and organization of lipid membranes—ions are always present in cationic lipid systems. The above examples demonstrate that detailed molecular dynamics studies can provide valuable insight into the atomistic organization of systems containing cationic lipids and yield useful information for experimentalists about the underlying mechanisms on the atomic and molecular levels.

In this work, our objective is to gain insight into the structural and electrostatic properties of cationic lipid bilayers through atomic classical molecular dynamics simulations. We concentrate on a bilayer mixture composed of two kinds of lipids: neutral (zwitterionic) DMPC and cationic DMTAP (see Fig. 1 for their chemical structures). Since DMTAP is positively charged under physiological conditions, we have neutralized its positive charges by chloride counterions. From the computational point of view, this choice for a model system is motivated by the fact that DMPC and DMTAP have the same nonpolar hydrocarbon chains and differ only by their headgroups. On the practical side, DMPC/DMTAP binary lipid mixtures have been widely studied in the presence of DNA by various experimental techniques (Artzner et al., 1998; Pohle et al., 2000; Zantl et al., 1999a,b), and also by computational methods (Bandyopadhyay et al., 1999).

We focus mostly on how the composition of the cationic lipid bilayer affects the structural and electrostatic properties
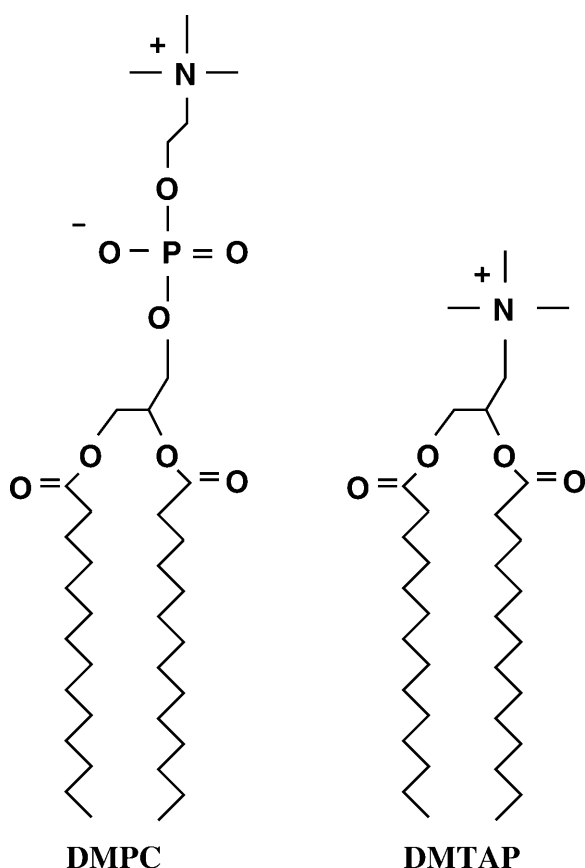
FIGURE 1   Chemical structures of the two lipids considered in this work: a zwitterionic dimyristoylphosphatidylcholine (DMPC) and a cationic dimyristoyltrimethylammonium propane (DMTAP).

of these lipid bilayer systems. To this end, we consider mixtures of DMPC and DMTAP with various different mole fractions of the cationic DMTAP component under conditions corresponding to the liquid-crystalline phase. We find that DMTAP plays a prominent role leading to considerable changes compared to the pure DMPC bilayer. As discussed in this study, this is characterized by the strong interplay between electrostatics and structural changes in the vicinity of the membrane-water interface. In particular, we find that DMTAP gives rise to a nonmonotonic dependence of the average area per lipid on the DMTAP concentration, substantial changes in the electrostatic profile of the membrane, and significant reorientation of P-N dipole vectors in DMPC headgroups. The spatial rearrangement of P-N dipoles is particularly interesting as it likely plays a significant role in the stability of DNA-membrane complexes.

SYSTEM

Model and simulation details

We have performed atomistic simulations of fully hydrated lipid bilayers consisting of a mixture of cationic DMTAP and zwitterionic DMPC lipids. In all simulations, the total number of lipid molecules was fixed to 128, and the number of water molecules ranged from 3527 (pure DMTAP) to 3655 (pure DMPC).

Force field parameters for the lipids were taken from the recent united atom force field (Berger et al., 1997). This force field has been previously validated (Lindahl and Edholm, 2000; Tieleman and Berendsen, 1996) and is essentially based on the GROMOS force field for lipid headgroups, the Ryckaert-Bellemans potential (Ryckaert and Bellemans, 1975, 1978) for hydrocarbon chains, and the OPLS parameters (Jorgensen and Tirado-Rives, 1988) for the Lennard-Jones interactions between united CH_n groups of acyl chains reparameterized for long hydrocarbon chains to reproduce experimentally observed values of volume per lipid (Nagle and Wiener, 1988). The parameters for this force field are available online at http://moose. bio.ucalgary.ca/Downloads/files/lipid.itp. Water was modeled using the SPC water model (Berendsen et al., 1981). The unit positive charge carried by each DMTAP molecule is compensated by the introduction of the corresponding number of explicit Cl^- counterions. Although being aware of the effects of different models for chloride (Patra and Karttunen, 2004), we decided to use the default set of chloride parameters supplied within the GROMACS force field (Berendsen et al., 1995; Lindahl et al., 2001).

Following the original parameterization (Berger et al., 1997), the Lennard-Jones interactions were cut off at 1 nm without shift or switch function. Since long-range electrostatic interactions are essential in this study, and since truncation of these interactions has been shown to lead to artifacts in simulations of phospholipid bilayers (Anézo et al., 2003; Patra et al., 2003; Tobias, 2001, and references therein), we employ the particle-mesh Ewald method (Darden et al., 1993). The long-range contribution to the electrostatics is updated every 10th time step.

The simulations were performed in the NPT ensemble. The temperature was kept constant using a Berendsen thermostat (Berendsen et al., 1984) with a coupling time constant of 0.1 ps. Lipid molecules and water (including counterions) were separately coupled to a heat bath. Pressure was controlled by a Berendsen barostat (Berendsen et al., 1984) with a coupling time constant of 1.0 ps. Pressure coupling was applied semiisotropically: The extension of the simulation box in the z direction (i.e., in the direction of the bilayer normal) and the cross-sectional area of the box in the x-y plane were allowed to vary independently of each other. Periodic boundary conditions were applied in all three dimensions.

We considered 11 DMPC/DMTAP mixtures ranging from pure DMPC to pure DMTAP. The molar fractions of the cationic DMTAP, χ_{TAP}, were taken to be 0.0, 0.06, 0.16, 0.25, 0.31, 0.39, 0.50, 0.63, 0.75, 0.89, and 1.0.

The hydration level used was essentially constant for all mixtures, ranging from 28.5 (pure DMPC bilayer) to 27.5 (pure DMTAP bilayer) water molecules per lipid. For comparison, Mashl et al. (2001) found recently that each headgroup in a pure dioleoylphosphatidylcholine bilayer can accommodate ~12 water molecules. Thus, we are confident that our DMPC bilayer is fully hydrated. As far as lipid bilayer mixtures are concerned, we excluded possible artifacts due to hydration (caused, e.g., by the binding of water molecules by Cl ions) by additional simulations with excess water: For DMTAP concentrations of 0.06, 0.50, and 0.75, we increased the number of water molecules by 50%. During multi-nanosecond simulations (~20 ns) we did not observe noticeable deviations in the structural properties discussed in this work (such as, e.g., the area per molecule).

The main transition temperature of a pure DMPC bilayer is $T_m = 24°C$ (Cevc and Marsh, 1987). For DMPC/DMTAP binary mixtures, it has been found (Zantl et al., 1999b) that the main transition temperature changes nonmonotonically with the mole fraction of DMTAP, demonstrating a maximum of ~37°C at $\chi_{TAP} \simeq 0.45$. All our simulations were done at a temperature of 50°C, such that the bilayers are in the liquid-crystalline phase.

All bond lengths of the lipid molecules were constrained to their equilibrium values using the LINCS algorithm (Hess et al., 1997) whereas the SETTLE algorithm (Miyamoto and Kollman, 1992) was used for water molecules. The time step in all simulations was set to 2 fs. All simulations were performed using the GROMACS package (Berendsen et al., 1995; Lindahl et al., 2001). The combined simulated time of all simulations amounts to 250 ns. Each simulation was run in parallel over four processors

on an IBM eServer Cluster 1600 system. In total, the simulations took ~20,000 h of CPU time.

Simulation setup

Mixtures of DMPC and DMTAP were prepared and equilibrated in several steps as follows:

1. We used the equilibrated dipalmitoylphosphatidylcholine (DPPC) bilayer structure of Patra et al. (2003) as our initial configuration. The structure is available electronically at http://www.softsimu.org/downloads.shtml.

2. DPPC and DMPC molecules differ only by length of their tail. Thus, we created a DMPC bilayer by shortening the DPPC acyl chains by two hydrocarbons. This procedure does not disturb the acyl chain region or the water-lipid interface.

3. The next step was to compress the DMPC bilayer to eliminate the gap between leaflets created in the previous step. For this purpose a preequilibration run for 1 ns in the NPT ensemble was performed. After this, the gap between leaflets had disappeared, and the obtained DMPC bilayer structure was used as initial configuration for all DMPC/DMTAP mixtures described in the following.

4. The chemical structures of DMPC and DMTAP differ only by their headgroups (see Fig. 1). With that in mind, the following procedure was used to prepare mixtures. For each DMTAP concentration, the corresponding number of randomly chosen PC headgroups in a pure DMPC bilayer were converted to TAP headgroups (Bandyopadhyay et al., 1999). To neutralize the unit charges in DMTAP headgroups, randomly chosen water molecules were replaced by chloride ions while ensuring a minimum separation of 0.5 nm between ions. To retain symmetry between the two leaflets, each of them contains the same number of cationic DMTAP.

5. Since TAP headgroups occupy a smaller volume than those of DMPCs, a short 10 ps run in the NVT ensemble was performed to let the water molecules adjust at the lipid-water interface. This step completes preequilibration.

6. The actual equilibration runs were performed in the NPT ensemble. The needed equilibration times before actual production runs ranged from 10 ns to 20 ns depending on the DMTAP mole fraction. We concluded that equilibration was completed when the average area per lipid had become stable and fluctuated around its mean with a standard deviation not exceeding the standard deviation for a pure DMPC bilayer.

After equilibration, for each DMPC/DMTAP mixture, we performed a production run of 10 ns in the NPT ensemble to collect the data for analysis. Final structures of all DMPC/DMTAP mixtures are available online at http://www.softsimu.org/downloads.shtml.

RESULTS AND DISCUSSION

Area per lipid

The average area per lipid, $\langle A \rangle$, is one of the most fundamental characteristics of lipid bilayers (Nagle and Tristram-Nagle, 2000). Although being one of the rather few structural quantities that can be measured accurately from model membranes via experiments, it also plays a major role in a number of quantities, including the ordering of acyl chains and the dynamics of lipids in a bilayer. Further, from a computational point of view, it is highly useful as a means of monitoring the equilibration process.

Due to the lack of experimental data for the average area per lipid in binary DMPC/DMTAP bilayer mixtures, or in a pure DMTAP bilayer (apart from the low-temperature

phase (Lewis et al., 2001)), reproduction of the experimental data available for pure DMPC membranes is essential to validate our approach. To this end, let us first consider the temporal behavior of the area per lipid, $A(t)$, presented in Fig. 2. It shows that the obtained average area per lipid for a pure DMPC system has a value of $\langle A \rangle = 0.656 \pm 0.008$ nm^2. As for experimental data on the area per lipid, it is well known that the results can vary significantly (up to ~20%) depending on the method used (Nagle and Tristram-Nagle, 2000). In particular, for the DMPC bilayer at 50°C, values of 0.629 nm^2 (Nagle et al., 1996), 0.654 nm^2 (Petrache et al., 2000), and 0.703 nm^2 (Costigan et al., 2000) have been reported. Therefore, our findings for a pure DMPC bilayer are in good agreement with the experimentally observed values, thereby validating our model in this respect. As for the pure DMTAP bilayer, Lewis et al. (2001) have been able to extract the area per lipid in the low-temperature phase, finding $\langle A \rangle = 0.40$ nm^2 at 25°C. Studies of $\langle A \rangle$ above the main transition temperature are lacking, however.

We find that the average area per lipid shows a non-monotonic dependence on DMTAP mole fraction χ_{TAP}, with a pronounced minimum roughly at $\chi_{TAP} = 0.5$ (see Fig. 3). This behavior is not trivial, as modest amounts of the cationic DMTAP lead to a compression of the bilayer, whereas high concentrations lead to a major expansion of the membrane. More specifically we find that for $0 < \chi_{TAP} \lesssim 0.8$, the average area per lipid is smaller than the
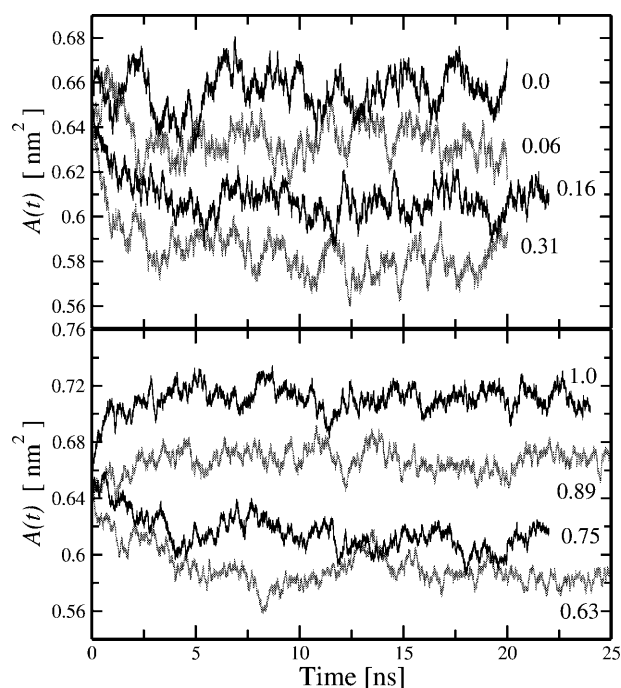
FIGURE 2 Time evolution of the area per lipid, $A(t)$, for different mixtures of DMPC and DMTAP. The low concentration results ($\chi_{TAP} \leq 0.31$) are shown on the top, and the high concentration regime ($\chi_{TAP} \geq 0.63$) is illustrated at the bottom. For clarity's sake, the results at intermediate concentrations are not shown here.
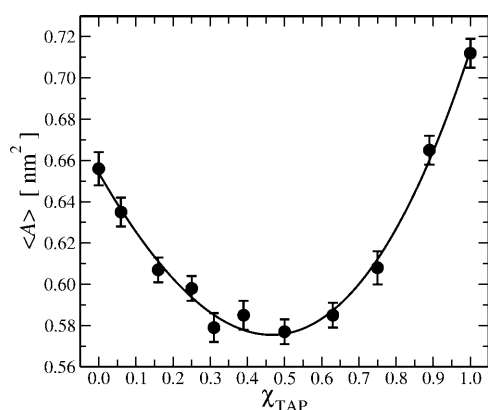
FIGURE 3 Average area per lipid $\langle A \rangle$ as a function of the DMTAP mole fraction, χ_{TAP}.

corresponding counterpart for any of the pure lipid systems. Such a behavior cannot be explained by steric interaction alone but most likely is rather of electrostatic origin.

Although no published experimental data exists (to the best of our knowledge) for the area per lipid of DMPC/DMTAP bilayer mixtures, similar behavior has been observed in related systems. For example, Zantl et al. (1999b) considered DMPC/DMTAP monolayers using Langmuir-type film balance and found that, for pressures corresponding to the liquid-crystalline phase, the headgroup area decreased monotonically for small χ_{TAP}, then had a minimum at about the equimolar ratio ($\chi_{TAP} \approx 0.5$), and increased for larger DMTAP mole fractions. This is in accord with our observations.

Another related work concerns Langmuir balance studies of mixed monolayers of zwitterionic palmitoyloleoylphosphatidylcholine (POPC) and cationic 2,3-dimethoxy-1,4-bis (N-hexadecyl-N;N-dimethyl-ammonium)butane dibromide (SS-1) (Säily et al., 2001). Although SS-1 is dicationic, one can qualitatively compare this system to our DMPC/DMTAP mixture. For the POPC/SS-1 system, Säily et al. (2001) found that the average area per lipid has a nonmonotonic behavior with a minimum at $\chi_{SS-1} \approx 0.38$. They also found that this effect depends on the charge of the headgroup, and it disappeared when POPC (having a zwitterionic headgroup) was replaced by neutral dioleylglycerol.

Our results in Fig. 3 suggest local extrema in $\langle A \rangle$ when χ_{TAP} is between 0.16 and 0.5 (in addition to global minimum at $\chi_{TAP} = 0.5$). In addition to the above-mentioned POPC and SS-1 study (Säily et al., 2001), similar and even more dramatic effects have been observed for mixtures of POPC and sphingosine (Säily et al., 2003). The existence of critical concentrations in lipid membranes has also been theoretically postulated by Somerharju et al. (Somerharju et al., 1999; Virtanen et al., 1998). In this case, the local extrema for DMPC/DMTAP mixtures are within error bars, and therefore may be interpreted as fluctuations of $\langle A \rangle$. To study such features in more detail, one needs to decrease the

fluctuations in the average area per lipid by, e.g., increasing the system size (Lindahl and Edholm, 2000). This, however, is beyond the scope of this study.

Nevertheless, we decided to approach this issue from a different perspective. To determine the average area per lipid separately for the two different components, we used the Voronoi tessellation technique in two dimensions (Patra et al., 2003). In Voronoi tessellation, we first calculated the center of mass (CM) positions for the lipids and projected them onto the x-y plane. A point in the plane is then considered to belong to a particular Voronoi cell, if it is closer to the projected CM of the lipid molecule associated with that cell than to any other CM position. As there is no unique definition for the area per molecule in a multi-component system, it is clear that the Voronoi results should be considered as suggestive rather than quantitative, providing insight mainly of the trends.

Fig. 4 demonstrates that the areas occupied by DMPC and DMTAP are distinctly different. For small χ_{TAP}, the area per DMPC is considerably larger than that of DMTAP. For larger DMTAP mole fractions above $\chi_{TAP} = 0.5$, the situation is the opposite. This behavior is related to electrostatic effects and the ordering of acyl chains, and will be discussed in more detail in the next section. Here we only note that the fluctuations in $\langle A \rangle$ (see Fig. 3) at $0.1 \lesssim \chi_{TAP} \lesssim 0.5$ arise from fluctuations in the area occupied by DMTAP. Whether this is a true result due to, e.g., clustering of lipids in this region remains to be resolved.

Ordering of lipid acyl chains

Ordering of nonpolar hydrocarbon chains in lipid bilayers is typically characterized by the deuterium order parameter S_{CD} measured through ^2H NMR experiments. If θ is the angle between a CD bond and the bilayer normal, the order parameter is defined as
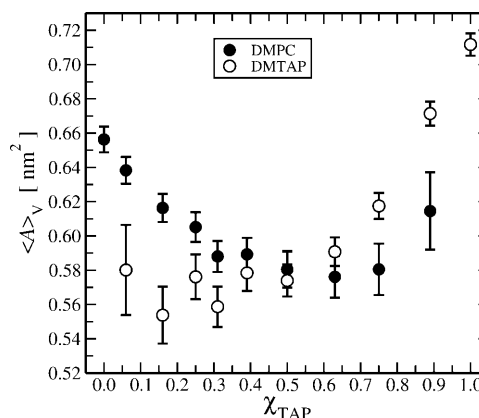

FIGURE 4 Average area per lipid $\langle A \rangle_V$ based on the Voronoi analysis in two dimensions. The results for DMPC and DMTAP are shown separately as a function of χ_{TAP}.

$$S_{CD} = \frac{3}{2}\langle\cos^2\theta\rangle - \frac{1}{2} \qquad (1)$$

separately for each hydrocarbon group. Since we employed a united atom force field, the positions of the deuterium atoms are not directly available but have to be reconstructed from the coordinates of three successive nonpolar hydrocarbons, assuming an ideal tetrahedral geometry of the central CH_2 group (Chiu et al., 1995; Hofsäss et al., 2003). In practice, we calculated S_{CD} following the standard approach described elsewhere (Patra et al., 2003).

Fig. 5 shows $|S_{CD}|$ averaged over the two similar atoms in the sn-1 and sn-2 chains, for both DMPC (*top*) and DMTAP (*bottom*) at different DMTAP concentrations. For the pure DMPC bilayer, we find $|S_{CD}| \approx 0.18$ close to the glycerol group of the molecule, in good agreement with recent experiments (Petrache et al., 2000) and molecular dynamics simulation studies (Róg and Pasenkiewicz-Gierula, 2001; Smondyrev and Berkowitz, 2001).

The order parameter profile for the first seven hydrocarbons (from C2 to C8) is a kind of plateau, and the average value of S_{CD} in this region, denoted by S_{ave}, is shown in Fig. 6. As expected, the results closely follow the change in the average area per lipid, i.e., a compression of the membrane is accompanied by enhanced ordering of nonpolar acyl chains. Results of similar nature have been observed, e.g., in bilayer mixtures of glycerophospholipids and cholesterol, where cholesterol both reduces the average area per molecule and enhances the ordering of lipid acyl chains (Hofsäss et al., 2003).

For pure DMPC, the plateau value S_{ave} equals 0.181 ± 0.009, which is in very good agreement with the experimentally measured value of 0.184 (Petrache et al., 2000). For
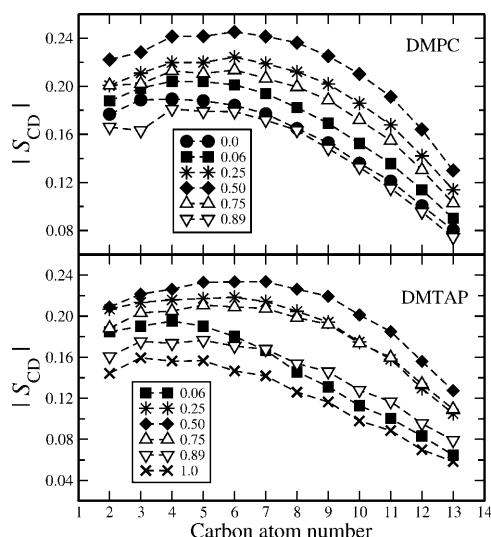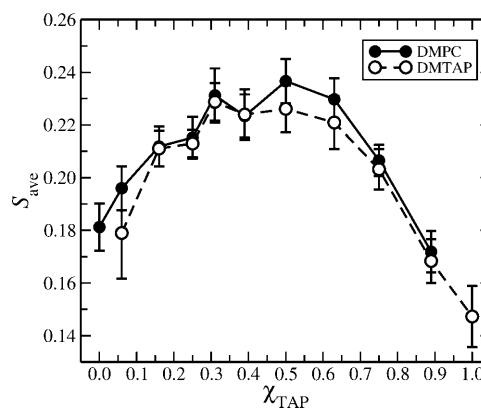

FIGURE 6 Plateau order parameter S_{ave} calculated by averaging S_{CD} over C2–C8 hydrocarbons. Shown are S_{ave} for DMPC (*solid lines* with *solid circles*) and DMTAP (*dashed lines* with *open circles*).

a pure DMTAP bilayer, the plateau value of S_{CD} is considerably smaller, being $\sim 0.147 \pm 0.011$. Therefore, chains in a pure DMTAP bilayer are on average more disordered than in a DMPC system, in agreement with our findings for $\langle A \rangle$.

Orientation of phosphatidylcholine headgroups

Since the chemical structures of the acyl chains of DMPC and DMTAP are identical, it is obvious that the differences between their behavior are due to their headgroups. Since the headgroup of DMPC is zwitterionic (cf. Fig. 1), it possesses a dipole moment along the P-N vector. The electrostatic potential across a monolayer thus depends sensitively on the distribution of the angle α between the P-N vector and the interfacial normal $\vec{n}$ (where $\vec{n}$ has been chosen to point away from the bilayer center along the z coordinate).

Fig. 7 shows the probability distribution function $P(\alpha)$ for the angle in question. For a pure DMPC bilayer, we find the distribution to be wide, thus allowing the P-N vector to fluctuate substantially, pointing at times in the direction of

FIGURE 5 Deuterium order parameter $|S_{CD}|$ averaged over sn-1 and sn-2 chains for DMPC (*top*) and for DMTAP (*bottom*) as a function of DMTAP mole fraction. Small carbon atom numbers correspond to those close to the headgroup.
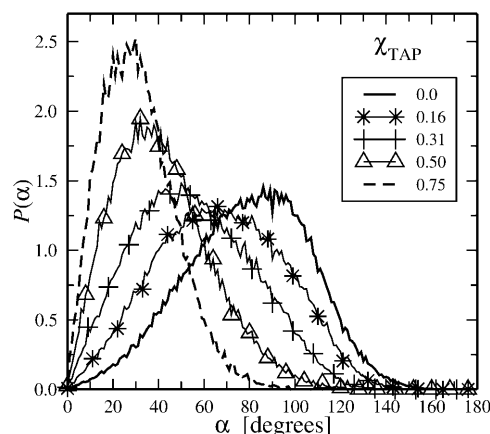

FIGURE 7 Results for the probability distribution function $P(\alpha)$ versus the angle α between the P-N vector (of DMPC headgroups) and the bilayer normal.

the membrane normal as well as into the bilayer interior. The average angle found in this case is $\sim(80 \pm 1)°$ (see Fig. 8), i.e., the PC heads are on average almost parallel to the membrane surface. This is in agreement with experimental observations (Hauser et al., 1981; Scherer and Seelig, 1989) as well as with recent computer simulations (Gabdoulline et al., 1996; Pasenkiewicz-Gierula et al., 1999; Smondyrev and Berkowitz, 1999).

Fig. 7 further reveals the major role played by DMTAP. The addition of even a small amount of DMTAP leads to a pronounced reorientation of the P-N dipole vector. As χ_{TAP} is increased, the profile of the distribution becomes considerably narrower and its maximum shifts to smaller angles. This trend continues up to the high-concentration limit $\chi_{TAP} \approx 0.75$, beyond which the distribution is essentially similar with the case found for $\chi_{TAP} = 0.75$.

Results for the average angle $\langle \alpha \rangle$ between the P-N vector and the membrane normal shown in Fig. 8 are consistent with this picture. On average, upon increasing χ_{TAP}, PC headgroups become more and more vertically oriented. Also this has been observed in several experiments (Scherer and Seelig, 1989; Säily et al., 2003, 2001; Zantl et al., 1999b). Moreover, our findings are in fairly good agreement with an atomistic MD study of a complex composed of DNA and a mixture of DMPC and DMTAP (Bandyopadhyay et al., 1999), in which the average angle between the P-N dipole vector and the bilayer normal was found to be $(50 \pm 8)°$ at an almost equimolar mixture of DMPC and DMTAP. In this case without DNA, we found $\langle \alpha \rangle = (42 \pm 2)°$ at $\chi_{TAP} = 0.5$.

Perhaps surprisingly, the correlation between the average area per lipid (Fig. 3) and the reorientation of the P-N dipole is not complete. As Fig. 8 shows, the reorientation extends by and large linearly up to $\chi_{TAP} = 0.75$, whereas the membrane compression completes at $\chi_{TAP} \approx 0.5$. This contradicts the conclusions of Säily et al. (2001), who studied POPC/

SS-1 cationic lipid mixtures using the Langmuir balance technique and suggested that the maximal average angle between the P-N dipole vector and membrane surface is achieved at the cationic lipid concentration that corresponds to the point where the membrane compression ends.

A closer inspection of Figs. 3 and 8 shows that the observed reduction of the average area per molecule is likely related to the reorientation of PC dipoles, and this in turn is related to the role of electrostatic interactions between DMPC and DMTAP headgroups. To bridge the two issues, we propose the following schematic scenario. At small χ_{TAP} where the DMTAP molecules are far apart and their mutual interaction is rather weak, we essentially suggest that the role of DMTAP is to reorient the headgroups of those DMPC molecules that are beside a DMTAP molecule. This favors more dense packing at small χ_{TAP}, leading to a reduction in $\langle A \rangle$, and consequently to a minimum in the area per molecule at intermediate concentrations because for large χ_{TAP} the repulsive electrostatic interactions between TAP headgroups enforce $\langle A \rangle$ to be expanded.

To validate this scenario, we complemented our results in Fig. 7 by calculating the probability distribution function $P(\alpha)$ for those DMPC molecules that are nearest neighbors to DMTAP. As a criterion that a DMPC and a DMTAP form a pair, we monitored the distance between PC phosphorus and TAP nitrogen. For that, we first calculated the radial distribution functions (RDFs) between pairs of P_{PC} and N_{TAP} and determined the distance r_{nn} at which the RDF had its first minimum after the main peak (see also ''Radial distribution functions and coordination numbers'' below). The distance obtained in this fashion ($r_{nn} \approx 0.665$ nm) (and found not to depend on χ_{TAP}) was applied to identify the DMPCs residing next to a DMTAP. As shown in Fig. 8, the reorientation of the P-N vector of these DMPCs is considerably stronger at small DMTAP concentrations as compared to that averaged over all DMPC lipids.

The above results imply that at small χ_{TAP}, the effect of DMTAP on the reorientation is mainly local, i.e., the alternating PC and TAP headgroups pack more tightly than in a pure DMPC system. This idea is supported by the results for the radial distribution functions discussed in ''Radial distribution functions and coordination numbers''. Beyond the small χ_{TAP} regime, for intermediate concentrations $0.3 \lesssim \chi_{TAP} \lesssim 0.5$, further increase in the concentration of DMTAP continues to increase the number of units composed of PC and TAP heads, thus favoring a reduction in $\langle A \rangle$. However, as repulsive electrostatic interactions between DMTAP molecules also become more and more important, the two effects compensate each other and $\langle A \rangle$ is found to be approximately constant. Finally, for large χ_{TAP}, the repulsive electrostatic interactions between TAP groups dictate the case discussed here and lead to an enhancement of the average area per molecule.

Though this picture does not account for the explicit influence of counterions, it grasps the essence of the process.
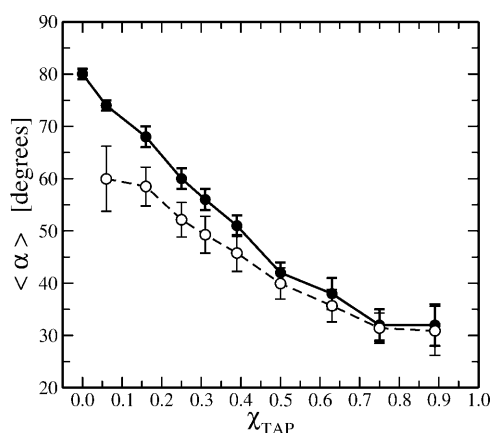

FIGURE 8   The average angle $\langle \alpha \rangle$ between the P-N vector of DMPC and the bilayer normal, shown as a function of DMTAP mole fraction. (●) Results averaged over all DMPC molecules in a given system. (○) Results averaged over only those DMPC molecules that are beside DMTAP. See text for details.

The effect of counterions is discussed separately in ''Radial distribution functions and coordination numbers''.

Density profiles of lipid headgroups and chloride ions

To quantify the locations of charge groups and counterions, we computed the density profiles across the bilayer, separated into the different constituents of the system. The positions of all atoms in the system were determined with respect to the instantaneous center of mass position of the bilayer, exploiting mirror symmetry such that atoms with $z < 0$ were folded to $z > 0$ (the bilayer center being at $z = 0$).

Fig. 9 shows the scaled number densities $\rho_N(z)$ for a few selected cases. Additionally, we note that the essential information is given by the positions of the density maxima depicted in Fig. 10.

At small χ_{TAP}, the density maxima of the nitrogen and phosphorus atoms in the DMPC heads almost coincide (see Fig. 9). The density profile of nitrogen in DMPC is nevertheless broader and extends further out of the bilayer plane. For larger χ_{TAP}, the density profiles of phosphorus and nitrogen are distinctly separated, and nitrogen in particular extends rather deeply into the water phase. The TAP group
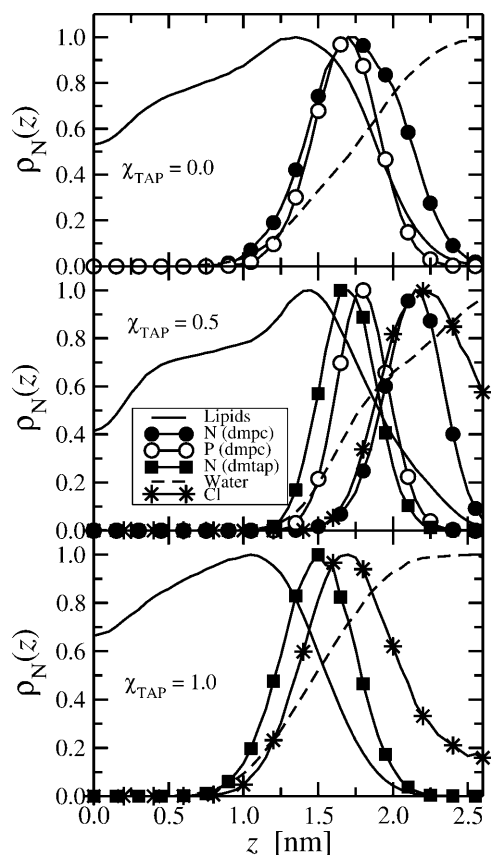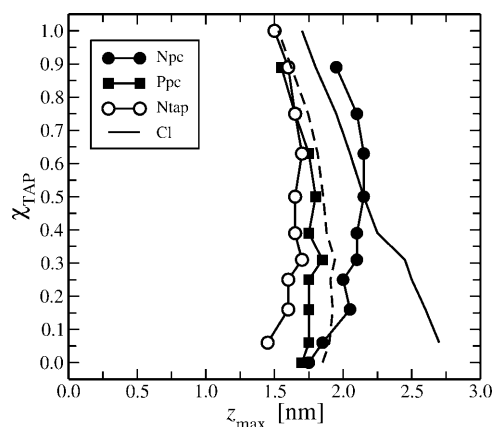

FIGURE 10 Maxima of the density profiles, z_{max}, for phosphorus and nitrogen atoms from the DMPC headgroups, and of the density profile of chloride ions. The maxima are shown for the z coordinate in the direction of the membrane normal, shown as a function of DMTAP molarity. The dashed line marks the position of the membrane-water interface determined from the condition that the densities of water and lipids (in Fig. 9) are equal.

represented by the nitrogen atom, however, is found to be deep in the bilayer. It seems obvious that these two issues are related, i.e., the density profiles of nitrogens in PC and TAP groups are well separated due to the electrostatic repulsion that essentially leads to the reorientation of PC headgroups. These results are hence consistent with those in the prior section and reflect the dependence of DMPC headgroup orientation on χ_{TAP}.

Interestingly, although being attracted by the DMTAP headgroups, the chloride anions cannot penetrate the outer boundary of the bilayer formed by the DMPC choline groups. This is in a sense to be expected since the DMPC headgroup is longer than the TAP group and thus extends further outward from the bilayer. There is thus a significant amount of shielding of the chloride ions in the presence of DMPC. Only for an almost pure DMTAP bilayer the chloride ions are located in the vicinity of the TAP headgroups.

Charge density, electrostatic potential, and orientation of water

The charge distribution shown in Fig. 11 was calculated in the same fashion as the density profiles. The results are clearly reminiscent of the density profiles in Fig. 9 and demonstrate the competition between charged PC and TAP groups, Cl anions, and water. The role of the TAP group is prominent.

From the charge densities, we also computed the electrostatic potential across the bilayer. The results are shown in Fig. 12, where the potential at the center of the bilayer has been set to zero. For a pure DMPC bilayer we obtain -0.578 V, which is in agreement with previous MD simulation studies (Chiu et al., 1995; Gabdoulline et al., 1996; Smondyrev and Berkowitz, 1999). Experimental data for phospholipid membranes ranges from -0.2 V to -0.6 V
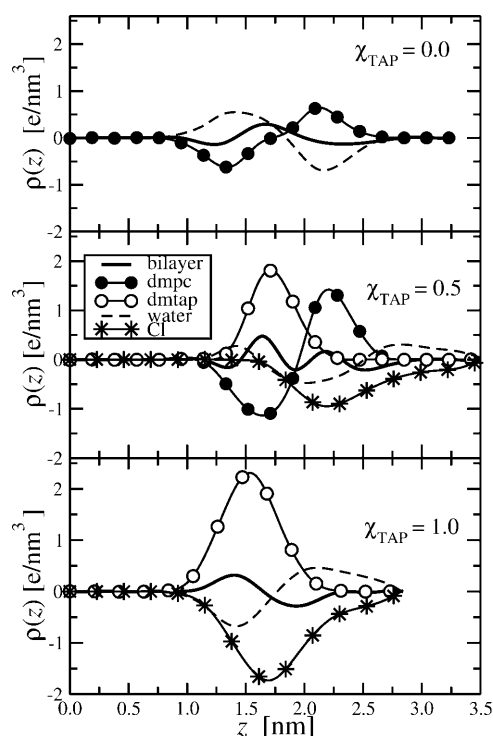

FIGURE 9 Scaled number densities $\rho_N(z)$ for three DMPC/DMTAP mixtures with $\chi_{TAP} = 0.0$ (*top*), $\chi_{TAP} = 0.5$ (*middle*), and $\chi_{TAP} = 1.0$ (*bottom*). The case $z = 0$ corresponds to the center of the bilayer.

FIGURE 11 Charge densities $\rho(z)$ across a single leaflet for χ_{TAP} equal to 0.0 (*top*), 0.5 (*middle*), and 1.0 (*bottom*). The case $z = 0$ corresponds to the center of the bilayer. Charge densities are shown as solid lines. In addition, the componentwise contributions due to DMPC (●), DMTAP (○), water (*dashed line*), and chloride ions (∗) are displayed. To reduce the noise in the data, the charge densities shown here were first fitted to splines (Thijsse et al., 1998). The error bars are of the same size as the symbols.

(Clarke, 2001; Flewelling and Hubbel, 1986; Gawrisch et al., 1992; Hladky and Haydon, 1973; Pickard and Benz, 1978).

The charge of the DMTAP headgroup is mainly compensated by, depending on the value of χ_{TAP}, chloride ions or DMPC phosphate groups. Most of the electrostatic potential across the bilayer thus is not due to the DMTAP itself but rather due to the reorientation of the DMPC
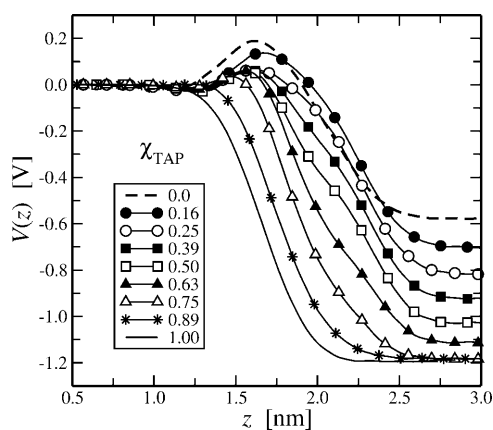
headgroups. A clear indication of this is that the potential build-up saturates at $\chi_{TAP} \simeq 0.75$, i.e., at the same value at which the distribution of headgroup orientation saturates (see Fig. 8). The total potential of the bilayer increases with increasing DMTAP concentration, with a difference of 0.6 V between pure DMPC and pure DMTAP. This increase agrees well with the experimental data on cationic POPC/SS-1 monolayers (Säily et al., 2001), and the authors offer the same explanation for their observations.

Many of the conclusions drawn from the charge density already follow from the number densities presented in the prior section, since for charged particles number density and charge density are trivially related. Water, however, has an additional internal degree of freedom, and a quick discussion of the orientation of the water molecules seems appropriate. As seen from Fig. 13, the average direction of the water dipoles in the membrane-water interface region is inverted for $\chi_{TAP} = 0.5 \rightarrow \chi_{TAP} = 1.0$. This is closely related with the familiar "hump" close to the interface, which is due to a subtle imbalance between the orientation of the water molecules and lipid headgroups (Chiu et al., 1995). At higher DMTAP concentrations, this "hump" disappears. A related issue concerns the pure DMTAP bilayer, in which case the density profile of water penetrates rather deep into the membrane (see Fig. 9), extending up to the interface region between the polar TAP group and the hydrophobic core. This is in accord with the interpretation of Fourier transform infrared spectroscopic measurements by Lewis et al. (2001).

Radial distribution functions and coordination numbers

To characterize the structure of the membrane-water interface region in more detail, we computed various RDFs among the atoms in the headgroups, Cl, and the oxygens. Here we briefly discuss the most relevant results.
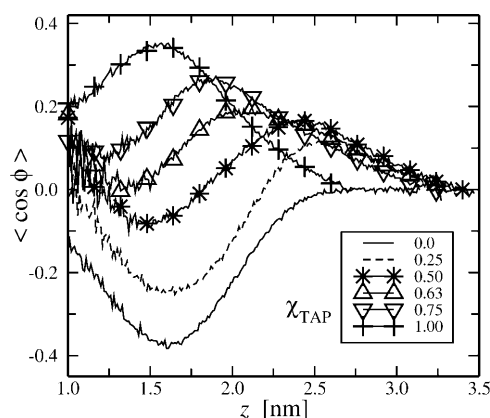

FIGURE 12 Electrostatic potential $V(z)$ across cationic bilayers at different DMTAP mole fractions.

FIGURE 13 Projection of the water dipole unit vector $\vec{\mu}(z)$ onto the interfacial normal $\vec{n}$, yielding $P(z) \equiv \langle \vec{\mu}(z) \cdot \vec{n} \rangle = \langle \cos \phi \rangle$. Here, $z = 0$ corresponds to the center of the bilayer, and the bilayer normal $\vec{n}$ is chosen to point away from the bilayer center.

The RDFs between the center of mass positions indicated that the leading (main) peak for DMPC-DMPC and DMTAP-DMTAP pairs was rather broad and at ~1.0 nm (data not shown). For DMPC-DMTAP pairs, however, the main peak of the RDF was much closer, at ~0.7 nm. This supports the conclusion made in ''Orientation of phosphatidylcholine headgroups'', i.e., DMPC and DMTAP form units that allow more dense packing than in a pure DMPC bilayer.

The N_{PC}-N_{PC} and N_{TAP}-N_{TAP} pairs were found to be rather far apart, the position of their main peak being at ~0.83 nm, whereas the N_{PC}-N_{TAP} pair was slightly closer (0.8 nm). The positions of the main peaks did not depend on χ_{TAP}. As for the RDFs of the phosphorus atoms in the PC headgroups, its main peak with respect to N_{PC} and N_{TAP} was found to be at a much closer distance, at 0.465 nm for N_{PC} and 0.485 nm for N_{TAP}. Again, the positions of these peaks did not depend on the DMTAP concentration.

We also calculated the coordination numbers for the phosphorus and nitrogen atoms at different DMTAP concentrations. These are shown in Fig. 14 (top). It turns out that in the range from $\chi_{TAP} = 0$ to 0.75, the PC nitrogens are to an increasing extent being replaced by N_{TAP} in the vicinity of P. This has twofold consequences: First, the electrostatic attraction between N^+ (TAP) and P^- (PC) enhances the compression of the bilayer for $0.0 < \chi_{TAP} \lesssim 0.5$ (see Fig.

3). Second, the decreasing coordination number for P-N_{PC} with χ_{TAP} supports the view that the DMPC nitrogens are pushed toward water, thereby PC headgroups are reoriented to a more vertical alignment with respect to the membrane plane (Fig. 8).

We conclude this section with a discussion of the location of chloride counterions. The positions of the main peaks of the RDFs for both types of nitrogens (in PC and TAP groups) with respect to Cl ions are identical, ~0.475 nm, and do not depend on χ_{TAP} (data not shown). In Fig. 14 (bottom), we plot the coordination numbers of chlorides in the vicinity of both types of nitrogens as a function of DMTAP concentration. The figure confirms that Cl ions are preferentially bound to PC nitrogens rather than to N_{TAP}. This holds up to a DMTAP mole fraction of ~0.75. The explanation for this is straightforward: as χ_{TAP} increases, the PC headgroups become more and more vertically oriented with respect to the bilayer plane. This, in turn, makes PC nitrogens more easily accessible for the Cl ions. In contrast, small TAP heads are located much deeper in the membrane surface region than the PC heads and therefore are able to attract fewer chlorides regardless of the fact that TAP heads carry a net positive charge. Interestingly, when the reorientation of PC heads is accomplished (at $\chi_{TAP} \approx 0.75$), the coordination number for N_{PC}-Cl pairs seems to saturate (see Fig. 14, bottom).

SUMMARY AND CONCLUSIONS

Drug delivery and gene therapy have attracted substantial interest due to their importance in treating human diseases. As far as experimental work is concerned, particular attention has been paid to nonviral delivery vectors such as cationic liposomes characterized by a number of desired properties such as high efficiency and lack of toxicity. Consequently, it is surprising how little is known about the atomic-level details of cationic lipid bilayers. Essentially, this is due to the lack of molecular simulations of these systems, the study by Bandyopadhyay et al. (1999) being the only exception, to the authors' knowledge, in this regard.

As a first step toward a detailed understanding of cationic membrane-DNA complexes on an atomic level, we have employed extensive molecular dynamics simulations of lipid bilayer mixtures composed of cationic DMTAP and neutral (zwitterionic) DMPC. Such binary DMPC/DMTAP mixtures have been studied widely through experiments, and have been shown to form stable complexes with DNA (Artzner et al., 1998; Pohle et al., 2000; Zantl et al., 1999a,b). In this work, we have focused on the influence of the composition of the cationic bilayer on its structural and electrostatic properties. For this purpose, we studied numerous DMPC/DMTAP mixtures in the liquid-crystalline phase by varying the mole fraction of DMTAP, χ_{TAP}, from the pure DMPC to the pure DMTAP bilayer.

We have found that the properties of the DMPC/DMTAP bilayer mixture are largely dominated by the electrostatic
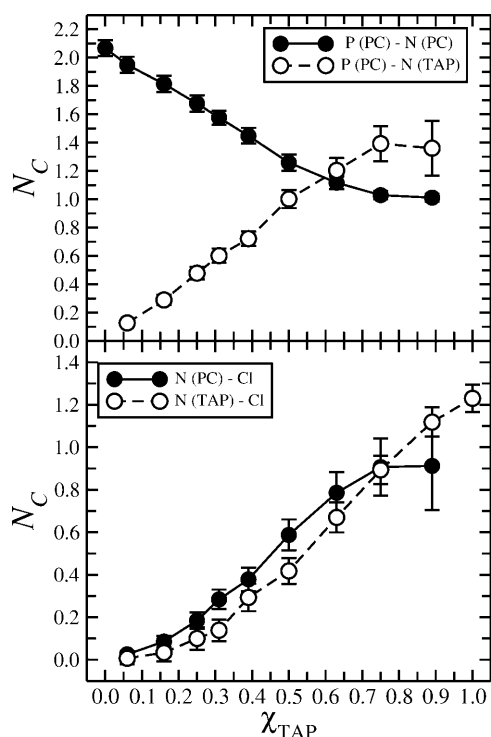

FIGURE 14 (Top) Coordination numbers N_C of DMPC phosphorus with DMPC nitrogen (solid line with solid circles) and with DMTAP nitrogen (dashed line with open circles) plotted versus χ_{TAP}. (Bottom) Coordination numbers N_C of DMPC nitrogen (solid line with solid circles) and DMTAP nitrogen (dashed line with open circles) with Cl ions.

properties of the headgroup region around the membrane-water interface. Most notably, our results indicate that there is a strong interplay between the PC and TAP groups together with the Cl counterions that concentrate in the vicinity of the bilayer-water interface.

The interplay between the PC and TAP groups leads to a number of intriguing observations. The key factor here is the reorientation of PC groups due to an introduction of DMTAP in the bilayer. The reorientation of the PC headgroups arises from electrostatic interactions that lead phosphate and choline groups to rearrange their positions with respect to the cationic TAP. This effect is enhanced as χ_{TAP} is increased, and extends up to large molar fractions of approximately $\chi_{TAP} = 0.75$. Beyond this limit, a further increase of DMTAP concentration has no additional effect on the orientation of PC headgroups. Interestingly, at small χ_{TAP} the effect of the reorientation is of local nature, i.e., the P-N dipoles of DMPCs beside DMTAP molecules reorient considerably.

At small molar fractions of DMTAP, the reorientation of PC dipoles leads to considerable compression of the bilayer, as alternating PC and TAP groups are able to pack more tightly than in a pure DMPC bilayer. The minimum of the area per lipid at $\chi_{TAP} \approx 0.5$ is ~12% smaller than in the pure DMPC bilayer. A further increase of χ_{TAP} leads to major expansion of the bilayer. This is essentially due to an increasing number of neighboring TAP groups whose cationic nature leads to repulsive electrostatic interactions that do not favor close packing. As expected, the ordering of acyl chains closely follows the change in the area per lipid. When these results are summarized, the view of the average area per lipid coupled to the reorientation of the headgroups can be summarized schematically as in Fig. 15.
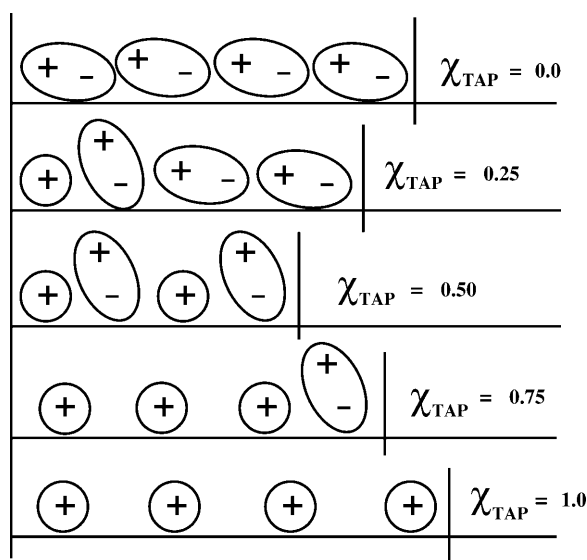
A problem commonly encountered in MD simulations of lipid bilayers is insufficient mixing of the different lipid components due to the limited length of the simulations. In this work, we found that the lateral diffusion coefficient was $\sim 1.4 \times 10^{-7}$ cm^2/s, leading to a diffusion length of $\sim$1.15 nm during a simulation of 22 ns. This is $\sim$1.5 times the diameter of a single lipid in the plane of the membrane, thus indicating that the lipid molecules in this study do mix rather well. In more general terms, dynamic properties of cationic lipid bilayers are of great importance on their own. However, such properties are beyond the scope of this work and will be discussed elsewhere.

In view of future studies of DNA-membrane systems, it is important to pay attention to the influence of DMTAP on the electrostatic properties of the membrane, including the increase in the electrostatic potential across the bilayer and the ordering of water in the vicinity of the membrane-water interface. Another often ignored aspect of electrostatics is that the ionic buffer liquids may affect membranes significantly (Böckmann et al., 2003).

Perhaps the most significant observation in this study is the spatial rearrangement of PC and TAP headgroups, which is expected to play a significant role in the condensation of DNA onto the membrane surface. The cationic TAP and choline groups then play a key role as the anionic phosphate groups of DNA come into contact with the membrane. Although this study clarifies some of the underlying questions related to binary mixtures of cationic and neutral (zwitterionic) lipid membranes, further atomic-level studies are essential to resolve other important issues related to DNA-membrane systems, such as the influence of salt and its screening effects, and the stability and interface properties under those conditions. Work in this direction is under way.

REFERENCES

Anderson, W. F. 1998. Human gene therapy. *Nature*. 392(Suppl.):25–30.

Anézo, C., A. H. de Vries, H. D. Höltje, D. P. Tieleman, and S. J. Marrink. 2003. Methodological issues in lipid bilayer simulations. *J. Phys. Chem. B*. 107:9424–9433.

Artzner, F., R. Zantl, G. Rapp, and J. O. Rädler. 1998. Observation of a rectangular columnar phase in condensed lamellar cationic lipid-DNA complexes. *Phys. Rev. Lett.* 81:5015–5018.

Astafieva, I., I. Maksimova, E. Lukanidin, V. Alakhov, and A. Kabanov. 1996. Enhancement of the polycation-mediated DNA uptake and cell transfection with pluronic P85 block copolymer. *FEBS Lett.* 389:278–280.

Bandyopadhyay, S., M. Tarek, and M. L. Klein. 1999. Molecular dynamics study of a lipid-DNA complex. *J. Phys. Chem. B*. 103:10075–10080.

FIGURE 15 A proposed schematic picture of the observed change in the area per lipid versus χ_{TAP}. Only headgroups of the lipids are shown here, and water (not shown) is above the headgroups.

Berendsen, H. J. C., J. P. M. Postma, W. F. van Gunsteren, A. DiNola, and J. R. Haak. 1984. Molecular dynamics with coupling to an external bath. *J. Chem. Phys.* 81:3684–3690.

Berendsen, H. J. C., J. P. M. Postma, W. F. van Gunsteren, and J. Hermans. 1981. Interaction models for water in relation to protein hydration. *In* Intermolecular Forces. B. Pullman, editor. Reidel, Dordrecht, The Netherlands. 331–342.

Berendsen, H. J. C., D. van der Spoel, and R. van Drunen. 1995. GROMACS: a message-passing parallel molecular dynamics implementation. *Comp. Phys. Comm.* 91:43–56.

Berger, O., O. Edholm, and F. Jahnig. 1997. Molecular dynamics simulations of a fluid bilayer of dipalmitoylphosphatidylcholine at full hydration, constant pressure, and constant temperature. *Biophys. J.* 72:2002–2013.

Böckmann, R. A., A. Hac, T. Heimburg, and H. Grubmüller. 2003. Effect of sodium chloride on a lipid bilayer. *Biophys. J.* 85:1647–1655.

Cevc, G., and D. Marsh. 1987. Phospholipid Bilayers: Physical Principles and Models. John Wiley & Sons, New York.

Chiu, S. W., M. Clark, V. Balaji, S. Subramaniam, H. L. Scott, and E. Jacobsson. 1995. Incorporation of surface tension into molecular dynamics simulation of an interface: a fluid phase lipid bilayer membrane. *Biophys. J.* 69:1230–1245.

Clarke, R. J. 2001. The dipole potential of phospholipid membranes and methods for its detection. *Adv. Colloid Interface Sci.* 89:263–281.

Costigan, S. C., P. J. Booth, and R. H. Templer. 2000. Estimations of lipid bilayer geometry in fluid lamellar phases. *Biochim. Biophys. Acta.* 1468:41–54.

Darden, T., D. York, and L. Pedersen. 1993. Particle mesh Ewald: an N log(N) method for Ewald sums in large systems. *J. Chem. Phys.* 98:10089–10092.

de Gennes, P.-G. 1999. Problems of DNA entry into a cell. *Physica A.* 274:1–7.

Feller, S. E. 2000. Molecular dynamics simulations of lipid bilayers. *Curr. Opin. Coll. Interface Sci.* 5:217–223.

Fischer, D., T. Bieber, Y. Li, H. Elsasser, and T. Kissel. 1999. A novel non-viral vector for DNA delivery based on low molecular weight, branched polyethylenimine: effect of molecular weight on transfection efficiency and cytotoxicity. *Pharm. Res.* 16:1273–1279.

Flewelling, R. F., and W. L. Hubbel. 1986. The membrane dipole potential in a total membrane potential model. *Biophys. J.* 49:541–552.

Gabdoulline, R. R., G. Vanderkooi, and C. Zheng. 1996. Comparison of the structures of dimyristoylphosphatidylcholine in the presence and absence of cholesterol by molecular dynamics simulations. *J. Phys. Chem.* 100:15942–15946.

Gao, X., and L. Huang. 1996. Potentiation of cationic liposome-mediated gene delivery by polycations. *Biochemistry.* 35:1027–1036.

Gawrisch, K., D. Ruston, J. Zimmerberg, V. A. Parsegian, R. P. Rand, and N. Fuller. 1992. Membrane dipole potentials, hydration forces, and the ordering of water at membrane surface. *Biophys. J.* 61:1213–1223.

Hauser, H., I. Pascher, R. H. Pearson, and S. Sundell. 1981. Preferred conformation and molecular packing of phosphatidylethanolamine and phosphatidylcholine. *Biochim. Biophys. Acta.* 650:21–51.

Hess, B., H. Bekker, H. J. C. Berendsen, and J. G. E. M. Fraaije. 1997. LINCS: a linear constraint solver for molecular simulations. *J. Comput. Chem.* 18:1463–1472.

Hladky, S. B., and D. A. Haydon. 1973. Membrane conductance and surface potential. *Biochim. Biophys. Acta.* 318:464–468.

Hofsäss, C., E. Lindahl, and O. Edholm. 2003. Molecular dynamics simulations of phospholipid bilayers with cholesterol. *Biophys. J.* 84:2192–2206.

Jorgensen, W., and J. Tirado-Rives. 1988. The OPLS potential functions for proteins. energy minimizations for crystals of cyclic peptides and crambin. *J. Am. Chem. Soc.* 110:1657–1666.

Kukowska-Latallo, J. F., A. U. Bielinska, J. Johnson, R. Spindler, D. A. Tomalia, and J. Baker. 1996. Efficient transfer of genetic material into mammalian cells using starburst polyamidoamine dendrimers. *Proc. Natl. Acad. Sci. USA.* 93:4897–4902.

Langer, R. 1998. Drug delivery and targeting. *Nature.* 392(Suppl.):5–10.

Lewis, R. N. A. H., S. Tristram-Nagle, J. F. Nagle, and R. N. McElhaney. 2001. The thermodynamic phase behavior of cationic lipids: calorimetric, infrared spectroscopic and X-ray diffraction studies of lipid bilayer membranes composed of 1,2-di-O-myristoyl-3-*N,N,N*-trimethylamino-propane (DM-TAP). *Biochim. Biophys. Acta.* 1510:70–82.

Lindahl, E., and O. Edholm. 2000. Mesoscopic undulations and thickness fluctuations in lipid bilayers from molecular dynamics simulations. *Biophys. J.* 79:426–433.

Lindahl, E., B. Hess, and D. van der Spoel. 2001. GROMACS 3.0: A package for molecular simulation and trajectory analysis. *J. Mol. Model.* 7:306–317.

Mashl, R. J., H. L. Scott, S. Subramaniam, and E. Jakobsson. 2001. Molecular simulation of dioleoylphosphatidylcholine lipid bilayers at differing levels of hydration. *Biophys. J.* 81:3005–3015.

Miyamoto, S., and P. A. Kollman. 1992. SETTLE: an analytical version of the SHAKE and RATTLE algorithms for rigid water models. *J. Comput. Chem.* 13:952–962.

Mönkkönen, J., and A. Urtti. 1998. Lipid fusion in oligonucleotide and gene delivery with cationic lipids. *Adv. Drug Deliv. Rev.* 34:37–49.

Nagle, J. F., and S. Tristram-Nagle. 2000. Structure of lipid bilayers. *Biochim. Biophys. Acta.* 1469:159–195.

Nagle, J. F., and M. C. Wiener. 1988. Structure of lipid bilayers. *Biochim. Biophys. Acta.* 942:1–10.

Nagle, J. F., R. Zhang, S. Tristram-Nagle, W. Sun, H. I. Petrache, and R. M. Suter. 1996. X-ray structure determination of fully hydrated L_α phase dipalmitoylphosphatidylcholine bilayers. *Biophys. J.* 70:1419–1431.

Pasenkiewicz-Gierula, M., Y. Takaoka, H. Miyagawa, K. Kitamura, and A. Kusumi. 1999. Charge pairing of headgroups in phosphatidylcholine membranes: a molecular dynamics simulation study. *Biophys. J.* 76:1228–1240.

Patra, M., and M. Karttunen. 2004. Systematic comparison of force fields for microscopic simulations of NaCl in aqueous solutions: Diffusion, free energy of hydration and structural properties. *J. Comput. Chem.* 25:678–689.

Patra, M., M. Karttunen, M. T. Hyvönen, E. Falck, P. Lindqvist, and I. Vattulainen. 2003. Molecular dynamics simulations of lipid bilayers: major artifacts due to truncating electrostatic interactions. *Biophys. J.* 84:3636–3645.

Petrache, H. I., S. W. Dodd, and M. F. Brown. 2000. Area per lipid and acyl length distributions in fluid phosphatidylcholines determined by ^{2}H NMR spectroscopy. *Biophys. J.* 79:3172–3192.

Pickard, A. D., and R. Benz. 1978. Transport of oppositely charged lipophilic probe ions in lipid bilayer membranes having various structures. *J. Membr. Biol.* 44:353–376.

Pitard, B., O. Aguerre, M. Airiau, A. M. Lachages, T. Boukhnikachvili, G. Byk, C. Dubertret, C. Herviou, D. Scherman, J. F. Mayaux, and J. Crouzet. 1997. Virus-sized self-assembling lamellar complexes between plasmid DNA and cationic micelles promote gene transfer. *Proc. Natl. Acad. Sci. USA.* 94:14412–14417.

Pohle, W., C. Selle, D. R. Gauger, R. Zantl, F. Artzner, and J. O. Rädler. 2000. FTIR spectroscopic characterization of a cationic lipid-DNA complex and its components. *Phys. Chem. Chem. Phys.* 2:4642–4650.

Róg, T., and M. Pasenkiewicz-Gierula. 2001. Cholesterol effects on the phosphatidylcholine bilayer nonpolar region: a molecular simulation study. *Biophys. J.* 81:2190–2202.

Ryckaert, J. P., and A. Bellemans. 1975. Molecular dynamics of liquid *n*-butane near its boiling point. *Chem. Phys. Lett.* 30:123–125.

Ryckaert, J. P., and A. Bellemans. 1978. Molecular dynamics of liquid alkanes. *Chem. Phys. Lett.* 66:95–106.

Saiz, L., S. Bandyopadhyay, and M. L. Klein. 2002. Towards an understanding of complex biological membranes from atomistic molecular dynamics simulations. *Biosci. Rep.* 22:151–173.

Saiz, L., and M. L. Klein. 2002. Computer simulation studies of model biological membranes. *Acc. Chem. Res.* 35:482–489.

Scherer, P. G., and J. Seelig. 1989. Electric charge effects on phospholipid headgroups. Phosphatidylcholine in mixtures with cationic and anionic amphiphiles. *Biochemistry.* 28:7720–7728.

Säily, V. M. J., J. M. Alakoskela, S. J. Ryhänen, M. Karttunen, and P. K. J. Kinnunen. 2003. Characterization of sphingosine-phosphatidylcholine monolayers: effects of DNA. *Langmuir.* 19:8956–8963.

Säily, V. M. J., S. J. Ryhänen, J. M. Holopainen, S. Borocci, G. Mancini, and P. K. J. Kinnunen. 2001. Characterization of mixed monolayers of phosphatidylcholine and a dicationic gemini surfactant SS-1 with a Langmuir balance: effects of DNA. *Biophys. J.* 81:2135–2143.

Smedt, S. C. D., J. Demeester, and W. E. Hennink. 2000. Cationic polymer based gene delivery systems. *Pharm. Res.* 17:113–126.

Smondyrev, A. M., and M. L. Berkowitz. 1999. Molecular dynamics simulation of fluorination effects on a phospholipid bilayer. *J. Chem. Phys.* 111:9864–9870.

Smondyrev, A. M., and M. L. Berkowitz. 2001. Molecular dynamics simulation of the structure of dimyristoylphosphatidylcholine bilayers with cholesterol, ergosterol, and lanosterol. *Biophys. J.* 80:1649–1658.

Somerharju, P., J. A. Virtanen, and K. H. Cheng. 1999. Lateral organisation of membrane lipids. The superlattice view. *Biochim. Biophys. Acta.* 1440:32–48.

Thijsse, B. J., M. A. Hollanders, and J. Hendrikse. 1998. A practical algorithm for least-squares spline approximation of data containing noise. *Comput. Phys.* 12:393–399.

Tieleman, D. P., and H. J. C. Berendsen. 1996. Molecular dynamics simulations of a fully hydrated dipalmitoylphosphatidylcholine bilayer with different macroscopic boundary conditions and parameters. *J. Chem. Phys.* 105:4871–4880.

Tieleman, D. P., S. J. Marrink, and H. J. C. Berendsen. 1997. A computer perspective of membranes: molecular dynamics studies of lipid bilayer systems. *Biochim. Biophys. Acta.* 1331:235–270.

Tobias, D. J. 2001. Electrostatics calculations: recent methodological advances and applications to membranes. *Curr. Opin. Struct. Biol.* 11:253–261.

Virtanen, J. A., K. H. Cheng, and P. Somerharju. 1998. Phospholipid composition of the erythrocyte membrane can be rationalized by a lipid head group superlattice-model. *Proc. Natl. Acad. Sci. USA.* 95:4964–4969.

Zantl, R., F. Artzner, G. Rapp, and J. O. Rädler. 1999a. Thermotropic structural changes of saturated-cationic-lipid-DNA complexes. *Europhys. Lett.* 45:90–96.

Zantl, R., L. Baicu, F. Artzner, I. Sprenger, G. Rapp, and J. O. Rädler. 1999b. Thermotropic phase behavior of cationic lipid-DNA complexes compared to binary lipid mixtures. *J. Phys. Chem. B.* 103:10300–10310.